

Enhanced FREFLO: Modeling of Congested Environments

AJAY K. RATHI, EDWARD B. LIEBERMAN, AND MARK YEDLIN

Preliminary work with the FREFLO macroscopic freeway traffic simulation model has revealed some limitations in the model's ability to realistically simulate some congested flow conditions. The formulation and implementation of an approach that modifies FREFLO so as to address these limitations is described. This approach yields realistic simulation results for moderate, as well as severe, congested flow conditions. The basic formulation of FREFLO and the modifications under this approach are presented. The problems observed under congested flow conditions are described and simulation results from test networks are shown.

FREFLO, developed by Payne (1), is a macroscopic simulation model of freeway traffic. The model is useful for the analysis of freeway operations because it allows users to simulate a wide range of freeway conditions at modest cost. Thus, it is possible to quantify the effects of projected changes in travel demand, as well as those from proposed operational improvements.

Use of FREFLO in several applications has shown that the model is limited in its ability to realistically simulate congested flow conditions. Various approaches have been suggested by Payne and others to resolve this limitation. The approaches require either some special user inputs for the congested freeway sections (2) or more substantial computing time (3).

With support from FHWA, a new approach to this problem was formulated and implemented. The approach described in this paper permits a realistic simulation under moderately, as well as severely, congested flow conditions. At the same time, no foreknowledge of congested locations or special user inputs are required. The approach also preserves the computational efficiency of FREFLO.

BACKGROUND

FREFLO simulates the flow of traffic on freeway networks using an aggregate variable formulation based on suitably modified analogies of fluid flow. The model, successor to MACK II, was developed to evaluate the consequences of different designs, expressed in terms of traffic operational measures of effectiveness.

Initial work with this model revealed that FREFLO was limited in its ability to realistically simulate congested flow conditions (1). This problem was traced to the discontinuity in the flow-density relationship at the onset of congested conditions and to the transformation of the model's formulation from continuous to discrete domain for implementation on a computer.

Payne (2) addressed this problem with some modifications to the equilibrium speed-density relationship, calibration of dy-

namic interaction parameters, and by provision of a discontinuous, speed-density relationship. Preliminary tests with these modifications produced satisfactory results under moderately congested conditions. Problems were still evident under severely congested conditions.

Babcock et al. (3) suggested a more fundamental approach to alleviate this problem—spatial discretization of the congested flow sections. Using a test network with bottleneck conditions, it was shown that the simulation accuracy depended on the length of the spatial steps and that very small spatial steps were required to realistically simulate congested conditions. Because such a discrete model would require excessive computing time, two adaptive schemes were presented: heuristic and natural.

The heuristic scheme places subdivisions within a subsection only where and when they are needed. Such determinations are made on the basis of geometry and flow level and are repeated at regular, user-set intervals so that the freeway is always properly, but not excessively, subdivided.

The arbitrary, often conservative, spatial discretization of the heuristic adaption can be avoided by a more natural adaption implemented through reformulation of the model into a Lagrangian (moving) reference frame. The Lagrangian reference frame differs from the Eulerian (stationary) reference frame of FREFLO in that all changes are measured relative to a particle in motion with the local flow. Due to this moving frame, the convection term in the FREFLO dynamic speed relationship is not needed. Thus, discretization becomes a natural part of the state equations.

These adaptive schemes were able to reduce the computing time to a fraction of the time required by the nonadaptive scheme. Of the two schemes, the natural adaption scheme was more accurate and efficient.

The FRECON model (3) was developed by implementing the heuristic adaption scheme in FREFLO. It was calibrated and validated using five peak period data sets from Santa Monica Freeway in Los Angeles. With the exception of a complex collector-distributor geometry, the simulation results were generally in agreement with the field data.

Although the spatial discretization approach is appealing, it has some limitations. Despite the adaptive scheme, the computing time requirements for proper discretization in large, congested networks can be costly. Furthermore, FRECON's ability to simulate severely congested flow conditions has not been demonstrated.

FREFLO itself is presently incorporated within the Traf (4) simulation system. The system allows FREFLO to interface with other simulation models that can represent neighboring arterials, urban streets, and rural road environments. Within the Traf system, an equilibrium traffic assignment model exists that may be used to provide volume and routing information to FREFLO.

The Traf system was developed and is supported under

contract to FHWA. It is currently in a limited distribution and has been used by both the Utah and Kansas Departments of Transportation to simulate traffic operations in complex freeway and street networks. During some simulation runs, unrealistically high densities were observed on links in the congested sections of the freeway network.

With support from FHWA, it was decided to modify the current formulation of FREFLO to address the observed deficiencies. These improvements were designed to be transparent to the user in both his input specifications and computer time requirements.

The basic FREFLO formulation and its recent improvements are presented in this paper. The problems observed under congested flow conditions are described. Test results are shown and compared with FRECON and the current version of FREFLO.

FREFLO

FREFLO is based on a continuum representation of traffic, described in terms of the following equations:

$$\frac{\partial \rho}{\partial t} + \frac{\partial q}{\partial x} = f(x, t) \quad (1)$$

$$\frac{\partial u}{\partial t} = u \frac{\partial u}{\partial x} - \frac{1}{T} \left[u - u_e(\rho) + v \frac{\partial \rho}{\partial x} \right] \quad (2)$$

[con-vection] [relaxation to equilibrium] [anticipation]

where

- $\rho(x, t)$ = density of vehicles,
- $u(x, t)$ = space-mean speed,
- $q(x, t)$ = flow rate,
- $f(x, t)$ = net flow entering freeway section,
- $u_e(\rho)$ = equilibrium speed-density relationship,
- T = relaxation coefficient,
- v = anticipation coefficient,
- x = position along the freeway, and
- t = time.

Equation 1 of the continuum formulation represents the conservation of vehicles. The variable $f(x, t)$ thus corresponds to on-ramp and off-ramp traffic. The dynamic speed-density relationship is contained in Equation 2. The three groups of terms in Equation 2 represent three components of the time rate of change of speed: (a) convection, the effect of vehicles from upstream arriving at this point; (b) relaxation to equilibrium, the effect of drivers adjusting their speeds to the equilibrium speed-density relationship; and (c) anticipation, the effect of drivers reacting to changing travel conditions ahead, that is, to (decrease, increase) speed in anticipation of (higher, lower) density downstream.

The discrete, computer implementable equations from the continuum formulation were derived by spatial averaging and Euler integration (5). Corresponding to the freeway section in Figure 1, the transformed equations are

Conservation:

$$\rho_j^{n+1} = \rho_j^n + \frac{\Delta t}{l_j \Delta x_j} \left[q_{j-1}^n + f_j^{on,n} - q_j^n - f_j^{off,n} \right] \quad (3)$$

Dynamic speed-density:

$$u_j^{n+1} = u_j^n + \Delta t \left[-u_j^n \frac{(u_j^n - u_{j-1}^n)}{\Delta x_j} - \frac{1}{T} \left(u_j^n - u_e(\rho_j^n) + v \frac{(\rho_{j+1}^n - \rho_j^n)}{\Delta x_j} \right) \right] \quad (4)$$

where

- n = current point in time (superscript);
- j = current section (subscript);
- l_j = number of lanes along section, j ;
- Δx_j = length of section, j ; and
- Δt = time step.

Equation 5 relates volume, density and speed under uniform conditions within a section.

Flow:

$$q_j^{n+1} = \rho_j^n u_j^n \quad (5)$$

This relationship is adapted from several alternatives primarily because of stability considerations (5). The terms "section" and "link" are used interchangeably.

Although Equations 3-5 form the basis of the simulation model, some modifications are required to make provisions for the links at the boundaries of freeway segments, that is, links with no adjoining upstream or downstream links. The boundary conditions are set as follows:

$$u_{j-1}^n = u_j^n \quad \text{if no adjoining upstream link}$$

$$\rho_{j+1}^n = \rho_j^n \quad \text{if no adjoining downstream link}$$

Some other modifications in computing upstream speed and downstream density—in the dynamic speed-density equation—are required to represent the general freeway subnetwork link of Traf (see Figure 2) wherein a link can have two feeder and two receiver links (6). This feature allows for the simulation of merging and diverging freeways.

For a general freeway link, the upstream speed and downstream density are computed as the weighted average of the flow according to the following relations:

$$\bar{u}_j^n = \frac{u_{f1}^{n-1} q_{f1}^{ou, n-1} P_{f1, j} + u_{f2}^{n-1} q_{f2}^{ou, n-1} P_{f2, j}}{q_j^{in, n-1}}; \quad (6)$$

$$q_j^{in, n-1} = 0$$

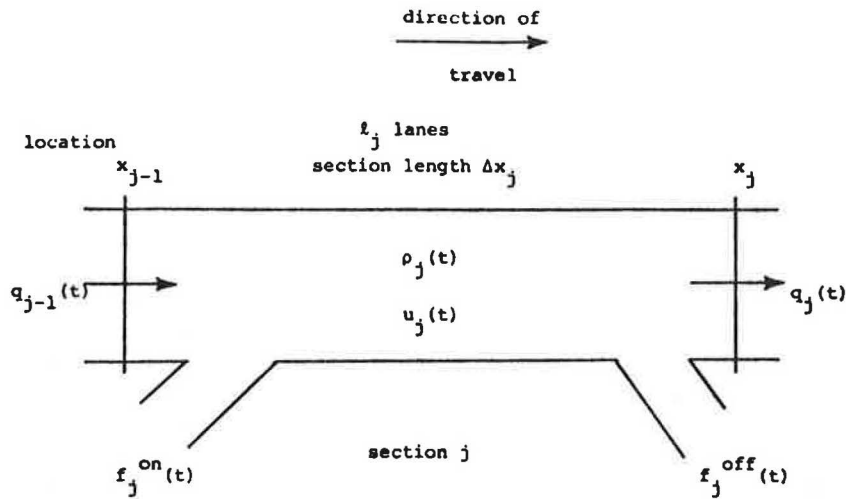


FIGURE 1 Freeway section depicting aggregate variables for a discrete formulation.

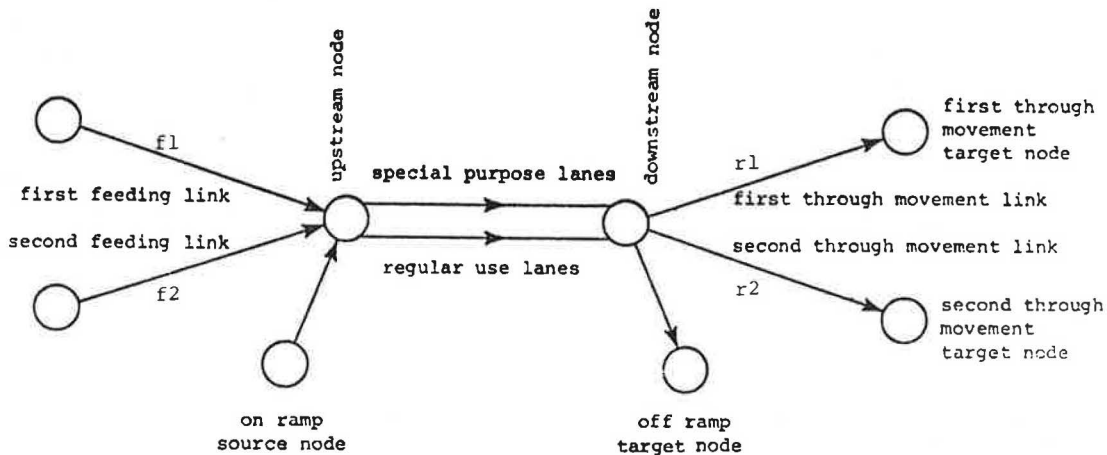


FIGURE 2 General freeway subnetwork link.

$$\bar{u}_j^n = 0; \quad q_j^{in, n-1} = 0 \quad (7)$$

$$\bar{\rho}_j^n = \frac{\rho_{r1}^{n-1} q_j^{out, n-1} P_{j, r1} + \rho_{r2}^{n-1} q_j^{out, n-1} P_{j, r2}}{q_j^{out, n-1}}; \quad q_j^{out, n-1} = 0 \quad (8)$$

$$\bar{\rho}_j^n = 0; \quad q_j^{out, n-1} = 0 \quad (9)$$

$q_j^{out, n}$ = exit flow rate on link j over time step n ,
 $\bar{\rho}_j^n$ = density of vehicles downstream of link j at the beginning of the time step n ,
 ρ_j^n = density of vehicles on link j at the end of time step n ,
 P_{ij} = fraction of flow rate of link i that enters link j ,
 f_1 = first feeding link,
 f_2 = second feeding link,
 r_1 = first receiving link, and
 r_2 = second receiving link.

where

\bar{u}_j^n = space-mean speed of vehicles upstream of link j at the beginning of time step n ,
 u_j^n = space-mean speed of vehicles on link j at the end of time step n ,
 $q_j^{in, n}$ = entry flow rate on link j over time step n ,

PROBLEMS

The departments of transportation in Utah and Kansas have been using Traf to simulate traffic operations on some large networks, which included arterials, freeways, and feeder streets. Due to capacity problems and demand pattern in the

freeway corridor, some sections of the freeway network experienced severe congestion. During simulation runs, FREFLO did not reflect the effects of these severely congested conditions as might be expected. Two problems were observed:

1. The densities on the congested freeway links were unrealistically high as more vehicles were allowed to enter a congested link than could be physically accommodated. Consequently, the congestion did not propagate upstream as expected.

2. In cases where one leg of a diverging freeway section experienced severe congestion, the density and entering volumes on the other noncongested leg were much lower than expected.

The simulation results in Table 1 from a test network shown in Figure 3 illustrate these problems. For this test network, the entry volume was set to 2,500 vehicles per hour (vph). The capacity of Sections 1–7 and 8–10 was set to 3,000 vph and 1,000 vph, respectively. The turn specifications from Section 5 to Sections 6 and 8 were such that the expected demand on Section 8 was 1,875 vph. With this demand, capacity flows were expected in Sections 8 through 10 and queuing on Section 5 and upstream. A time slice, Δt , of 4 sec was used.

Because the inflow rate exceeds the outflow capacity, the density on Section 8 increases with time (Table 1). The inflow rate starts to decrease as the feeder link (Section 5) responds to the downstream congestion by reducing the outflow. Due to this reduction in outflow, the density on Section 5 also increases with time.

After only 180 sec of simulation, the density on Section 8

reaches 252 vehicles per lane-mile, which is higher than attainable. This occurs because the anticipation term in the dynamic speed relationship (Equation 4) used by FREFLO underestimates the extent that speeds would be reduced in response to severe downstream congestion. After 260 sec, the outflow from Section 5 has dropped to zero and its density increases rapidly. Although discharge flow is terminated from Section 5, the flow entering downstream Sections 6 and 8 is not immediately reduced. Because volumes entering a section are computed at the beginning of a time slice, feeding flow may lag by one time slice if a link is processed before its feeder(s).

For the next time slice, Equation 9 is applied to compute the downstream density on Sections 6 and 8 as zero because the outflow rate from Section 5 is zero. As a consequence of this spurious result, Section 5 discharges vehicles to both Sections 6 and 8 to the maximum extent possible.

Also, the density on Sections 6 and 8 decreases because flow was terminated from Section 5 during the previous time slice. The indicated decrease in density in Section 6 is unrealistic because under these conditions only the flow entering the congested receiver (Section 8) should be reduced and not the flow entering Section 6. This result occurs because the current formulation of FREFLO does not consider the downstream density of each receiver separately when outflow is computed in a diverging scenario. Instead a single, weighted downstream density is computed based on the flow for each movement. This formulation allows maximum outflow from the feeding section, thereby increasing the density still further on the congested receiver. This problem is exhibited in Table 1 at time 280.

In the subsequent time slices, flow continues to enter Section 8 despite unrealistically high densities within the section. As a

TABLE 1 TEST NETWORK SIMULATION RESULTS—CURRENT FREFLO

| Time (sec) | q_5^{in} | q_5^{out} | ρ_5 | u_5 | q_6^{in} | q_6^{out} | ρ_6 | u_6 | q_8^{in} | q_8^{out} | ρ_8 | u_8 |
|------------|-------------------|--------------------|----------|-------|-------------------|--------------------|----------|-------|-------------------|--------------------|----------|-------|
| 60 | 2498 | 2419 | 23.2 | 45.2 | 605 | 598 | 6.0 | 50.3 | 1814 | 1048 | 119.0 | 8.0 |
| 120 | 2491 | 2347 | 30.6 | 36.9 | 590 | 583 | 6.3 | 46.2 | 1771 | 1030 | 187.3 | 5.2 |
| 180 | 2464 | 2117 | 40.1 | 24.1 | 547 | 540 | 6.5 | 40.9 | 1638 | 1019 | 251.5 | 3.9 |
| 190 | 2484 | 2441 | 42.8 | 21.5 | 529 | 443 | 6.5 | 39.8 | 1588 | 1012 | 260.6 | 3.8 |
| 200 | 2441 | 1930 | 45.7 | 18.4 | 504 | 468 | 5.9 | 38.7 | 1512 | 1015 | 267.2 | 3.7 |
| 210 | 2462 | 1764 | 49.4 | 14.9 | 482 | 475 | 6.2 | 37.6 | 1447 | 1012 | 274.5 | 3.6 |
| 220 | 2470 | 1548 | 54.5 | 10.7 | 441 | 446 | 6.2 | 36.2 | 1323 | 1008 | 280.8 | 3.5 |
| 230 | 2462 | 1195 | 61.3 | 5.8 | 387 | 414 | 6.2 | 34.7 | 1161 | 1004 | 285.5 | 3.5 |
| 240 | 2462 | 648 | 70.6 | 0.2 | 299 | 374 | 6.0 | 33.0 | 896 | 990 | 287.8 | 3.5 |
| 250 | 2448 | 14 | 83.9 | 0.1 | 162 | 302 | 5.4 | 31.1 | 486 | 983 | 286.4 | 3.5 |
| 260 | 2476 | 0 | 102.3 | 0.0 | 4 | 216 | 4.2 | 30.9 | 11 | 972 | 277.8 | 3.7 |
| 270 | 2412 | 1303 | 120.5 | 11.6 | 0 | 140 | 0.0 | 40.8 | 0 | 965 | 0.0 | 3.9 |
| 280 | 2362 | 2632 | 128.6 | 7.1 | 326 | 148 | 1.6 | 35.1 | 977 | 979 | 249.4 | 4.0 |
| 290 | 2333 | 1570 | 126.6 | 3.4 | 658 | 256 | 2.9 | 33.5 | 1974 | 1015 | 249.4 | 3.9 |
| 300 | 2354 | 1224 | 132.2 | 5.5 | 392 | 385 | 5.9 | 32.4 | 1177 | 1015 | 263.4 | 3.8 |
| 360 | 2290 | 1526 | 170.3 | 4.3 | 382 | 382 | 5.8 | 32.6 | 1141 | 1004 | 271.6 | 3.7 |
| 540 | 1519 | 1498 | 172.2 | 4.3 | 374 | 374 | 5.8 | 32.5 | 1123 | 1001 | 303.5 | 3.3 |
| 720 | 1523 | 1494 | 186.6 | 4.0 | 371 | 371 | 5.7 | 32.4 | 1112 | 997 | 335.5 | 3.0 |
| 900 | 1483 | 1483 | 187.7 | 4.0 | 371 | 371 | 5.8 | 32.3 | 1112 | 997 | 368.1 | 2.7 |

q_j^{in} = entry flow rate on link j (vehicles/hour) q_j^{out} = exiting flow rate on link j (vehicles/hour)

ρ_j = computed density on link j at the beginning of time slice (vehicles/lane-mile)

u_j = computed speed on link j at the end of time slice (miles/hour)

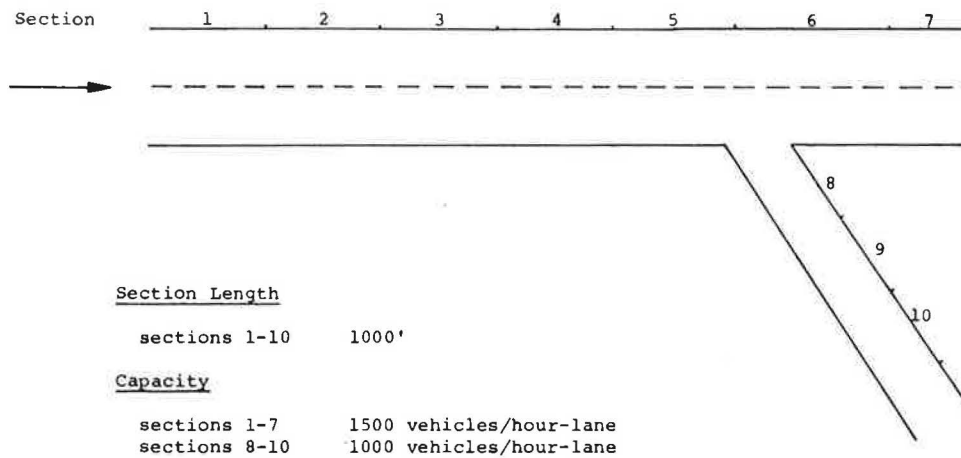


FIGURE 3 Nonlinear test network.

result, congestion propagates upstream much more slowly than expected. The entering volume and density on Section 6, on the other hand, are smaller than expected.

MODIFICATIONS TO FREFLO

The problem of excessively high densities on congested links was addressed through an approach that not only provides a sensible description of traffic operations during congested flow conditions but also eliminates the necessity of specific user inputs for congested freeway sections. The approach also preserves the computational efficiency of FREFLO. Under this approach, flow restrictions were implemented on the congested links and speeds were computed considering congestion on the links rather than using the dynamic speed equation of FREFLO. The densities, of course, were then computed from the conservation equation. Because the dynamic-speed-density equation is not used under severely congested conditions, recalibration and reformulation of FREFLO are not required.

The problems associated with the computation of flow rate for the case of imbalanced downstream density were addressed by weighting the downstream density effect of two discharging movements on the basis of overall turning percentage rather than on the instantaneous flow rates. This weighting scheme ensures that the computed densities reflect the actual conditions downstream of the section. The flow percentage-based weighting scheme is equivalent to the flow rate-based weighting scheme (Equation 8) as long as the outflow from the feeder section is not terminated.

The modifications are applied, in general, whenever the density of a section exceeds a prespecified congestion value, regardless of geometric configuration. In the absence of congestion, simulation is performed using the current FREFLO formulation. The modifications are described in detail elsewhere (7).

SIMULATION RESULTS

The simulation program was modified to include the special congestion scenarios described above. Under these modifications, the special treatment for congested links was applied whenever link density exceeded 120 vehicles per lane-mile. To

evaluate the effects of these modifications, traffic flow was simulated for both straight and diverging freeway sections. For both configurations, congestion was created with capacity constraints. The results are described in the following sections.

DIVERGING FREEWAY SECTION

After FREFLO was modified to incorporate the new congestion mechanism, simulation was again performed on the test network shown in Figure 3. The new results are presented in Table 2. Note that all figures represent values associated within a single time slice, Δt , of 4-sec duration; these are not time-averaged values.

In comparison with the original FREFLO results (Table 1), it is seen that the modified FREFLO produced much lower and more realistic densities in the congested Sections 5 and 8. The maximum value of density computed for any one time slice under the new logic was 152 vehicles per lane-mile compared with a maximum value of 368.1 vehicles per lane-mile under current FREFLO.

The congestion on Section 8 also propagates upstream to Section 5 much faster as a result of the modifications. As shown in Table 2, the outflow from Section 5 to Section 8 was reduced to zero at 70 sec of simulation after the density on Section 8 reached a congested level of 122 vehicles per lane-mile. In the original run (Table 1) outflow from Section 5 was not cut off in any time step until 270 sec of simulation; at that time the density on Section 8 had reached 278 vehicles per lane-mile.

With the new logic the density continued to build on Section 5 until it too became congested. Entry flow to Section 5 was ultimately reduced to zero at 220 sec of simulation. In the original run, the entry flow to Section 5 was never restricted to zero.

After Section 8 reached a congested density at 60 sec of simulation, a realistic stop-and-go pattern of entering flow was established under the modified FREFLO. This intermittent entry flow pattern was not observed in the original run.

In addition to these improvements for the congested links, the modified FREFLO also allowed a higher level of flow into uncongested Section 6. With the modifications, the density and entering volumes on Section 6 were less affected by the congestion on Section 8 than they had been under current

TABLE 2 VOLUME LEAVING SECTIONS (vehicles/hour)—CURRENT FREFLO

| Time (sec) | q_5^{in} | q_5^{out} | ρ_5 | u_5 | q_6^{in} | q_6^{out} | ρ_6 | u_6 | q_8^{in} | q_8^{out} | ρ_8 | u_8 |
|------------|------------|-------------|----------|-------|------------|-------------|----------|-------|------------|-------------|----------|-------|
| 30 | 2491 | 2419 | 24.6 | 48.3 | 605 | 590 | 5.7 | 51.9 | 1814 | 1062 | 88.9 | 10.6 |
| 40 | 2498 | 2419 | 25.1 | 47.2 | 605 | 598 | 5.8 | 51.3 | 1814 | 1055 | 99.9 | 9.5 |
| 50 | 2491 | 2412 | 23.7 | 46.1 | 605 | 598 | 5.9 | 50.7 | 1814 | 1051 | 111.0 | 8.6 |
| 60 | 2498 | 598 | 26.3 | 30.1 | 605 | 598 | 6.0 | 50.2 | 1811 | 1048 | 122.2 | 7.8 |
| 70 | 2491 | 605 | 40.2 | 22.4 | 598 | 562 | 6.0 | 42.8 | 0 | 983 | 133.4 | 7.9 |
| 80 | 2477 | 2639 | 54.1 | 27.7 | 605 | 526 | 6.2 | 39.3 | 0 | 936 | 119.0 | 8.9 |
| 90 | 2441 | 2898 | 52.9 | 29.4 | 659 | 558 | 6.8 | 41.1 | 1980 | 1004 | 105.2 | 8.9 |
| 100 | 2441 | 2884 | 49.5 | 31.4 | 724 | 644 | 7.6 | 42.0 | 2174 | 1062 | 119.5 | 7.8 |
| 110 | 2470 | 727 | 46.2 | 24.6 | 720 | 691 | 8.1 | 42.9 | 2164 | 1058 | 135.8 | 7.0 |
| 120 | 2984 | 727 | 59.0 | 20.2 | 727 | 698 | 8.3 | 40.2 | 0 | 994 | 152.0 | 6.9 |
| 130 | 2484 | 727 | 71.9 | 17.1 | 727 | 677 | 8.6 | 38.4 | 0 | 943 | 137.4 | 7.7 |
| 140 | 2441 | 727 | 84.7 | 14.9 | 727 | 684 | 8.9 | 37.1 | 0 | 936 | 123.5 | 8.6 |
| 150 | 2419 | 2905 | 97.3 | 15.7 | 724 | 684 | 9.2 | 36.3 | 0 | 929 | 109.7 | 9.7 |
| 160 | 2398 | 2927 | 93.7 | 16.4 | 727 | 698 | 9.6 | 36.5 | 2178 | 1012 | 96.0 | 9.5 |
| 200 | 2470 | 727 | 111.4 | 11.8 | 734 | 713 | 9.9 | 35.6 | 0 | 940 | 131.5 | 8.0 |
| 210 | 2426 | 2934 | 124.1 | 12.3 | 727 | 713 | 10.1 | 35.1 | 0 | 932 | 117.6 | 9.0 |
| 220 | 0 | 2826 | 120.4 | 13.7 | 734 | 720 | 10.2 | 35.3 | 2200 | 1015 | 103.9 | 8.8 |
| 300 | 2876 | 745 | 133.5 | 10.0 | 752 | 731 | 10.4 | 34.9 | 0 | 997 | 145.5 | 7.3 |
| 600 | 2506 | 634 | 99.4 | 11.3 | 637 | 671 | 9.8 | 35.4 | 0 | 990 | 140.0 | 7.6 |
| 900 | 2232 | 634 | 96.5 | 11.8 | 634 | 680 | 9.8 | 35.6 | 0 | 990 | 147.0 | 7.0 |

q_j^{in} = entry flow rate on link j (vehicles/hour) q_j^{out} = exiting flow rate on link j (vehicles/hour)

ρ_j = computed density on link j at the beginning of time slice (vehicles/lane-mile)

u_j = computed speed on link j at the end of time slice (miles/hour)

FREFLO. The traffic densities in Sections 1–10 under modified FREFLO are given in Table 3. The results show the spread of congestion upstream of Section 8 as expected. Such timely propagation of congestion to upstream sections was not observed under the current version of FREFLO.

Thus, the modified FREFLO allows for stop-and-go operations of traffic only onto the congested branch of a diverging freeway section. Neither the current FREFLO nor FRECON has such a response mechanism; that is, the flow is terminated to both receivers. Therefore, both FRECON and current FREFLO are limited in their applicability for diverging freeway sections operating under congested conditions.

LINEAR FREEWAY SECTION

This test section (Figure 4) was identical to the bottleneck geometry used by Babcock et al. (4) in their demonstration of the effect of spatial discretization. The traffic flow in this network simulated for a period of 10 min using both current FREFLO and its modified version. The lane capacity was set to 2,000 vph and entry volume was set to 4,500 vph. With this demand level and capacity specification, capacity flows were expected in Sections 6 through 10 and queuing on sections upstream of Section 6.

Tables 4 through 9 give the simulated output volumes and

TABLE 3 NONLINEAR TEST NETWORK SIMULATION RESULTS—MODIFIED FREFLO

| Time (min.) | Section | | | | | | | | | |
|-------------|---------|-------|-------|-------|-------|------|------|-------|------|------|
| | 1 | 2 | 3 | 4 | 5 | 6 | 7 | 8 | 9 | 10 |
| 1 | 24.0 | 23.9 | 23.7 | 23.8 | 40.2 | 6.0 | 5.6 | 133.4 | 48.9 | 30.5 |
| 2 | 24.0 | 23.9 | 23.8 | 25.1 | 71.9 | 8.6 | 6.9 | 137.4 | 59.0 | 38.2 |
| 3 | 24.0 | 23.9 | 23.9 | 28.0 | 98.6 | 9.9 | 7.8 | 146.1 | 63.5 | 44.5 |
| 4 | 24.0 | 23.9 | 25.4 | 67.3 | 102.9 | 9.9 | 8.0 | 122.2 | 68.1 | 49.8 |
| 5 | 24.0 | 23.9 | 25.9 | 69.6 | 149.1 | 10.6 | 18.0 | 130.8 | 71.5 | 54.3 |
| 6 | 24.0 | 24.7 | 69.2 | 94.1 | 116.8 | 9.8 | 8.1 | 106.2 | 73.7 | 58.0 |
| 7 | 24.0 | 26.0 | 50.5 | 117.7 | 149.5 | 10.4 | 8.1 | 113.5 | 76.2 | 61.8 |
| 8 | 24.0 | 45.4 | 138.3 | 102.2 | 112.3 | 9.3 | 7.9 | 117.0 | 78.7 | 64.9 |
| 9 | 32.2 | 94.2 | 79.6 | 87.0 | 126.1 | 10.1 | 7.9 | 123.1 | 81.3 | 67.8 |
| 10 | 40.7 | 109.3 | 118.7 | 93.5 | 93.5 | 9.5 | 8.0 | 125.5 | 82.4 | 70.4 |

TABLE 6 VOLUME LEAVING SECTIONS (vehicles/hour)—MODIFIED FREFLO

| Time (min.) | Section | | | | | | | | | |
|----------------|---------|------|------|------|------|------|------|------|------|------|
| | 1 | 2 | 3 | 4 | 5 | 6 | 7 | 8 | 9 | 10 |
| 1 | 4500 | 4500 | 4500 | 4500 | 4428 | 4068 | 3953 | 3877 | 3802 | 3773 |
| 2 | 4500 | 4500 | 4500 | 4540 | 4 | 4136 | 4010 | 3931 | 3877 | 3823 |
| 3 | 4500 | 4500 | 4500 | 4612 | 5677 | 4284 | 4003 | 3935 | 3899 | 3834 |
| 4 | 4500 | 4500 | 4201 | 4741 | 4975 | 3989 | 3848 | 3928 | 3899 | 3852 |
| 5 | 4500 | 4500 | 4597 | 5634 | 4 | 4194 | 3992 | 3910 | 3902 | 3881 |
| 6 | 4500 | 4500 | 4597 | 7 | 0 | 3269 | 3982 | 3924 | 3899 | 3877 |
| 7 | 4612 | 5022 | 5778 | 5576 | 4694 | 4133 | 3974 | 3895 | 3881 | 3888 |
| 8 | 4244 | 5522 | 4746 | 5335 | 4946 | 4108 | 3956 | 3920 | 3899 | 3888 |
| 9 | 3902 | 0 | 5314 | 4334 | 4579 | 3982 | 3942 | 3895 | 3877 | 3888 |
| 10 | 5065 | 4 | 4 | 5033 | 3791 | 4162 | 3827 | 3895 | 3913 | 3877 |

NOTE: These are instantaneous volumes of the indicated times over a time-step of four seconds.

TABLE 7 VOLUME (vehicles/hour) LEAVING SECTION 5—MODIFIED FREFLO

| Slice | Time (min.) | | | | | | | | | |
|-------------------------------|-------------|------|------|------|------|------|------|------|------|------|
| | 1 | 2 | 3 | 4 | 5 | 6 | 7 | 8 | 9 | 10 |
| 1 | 4442 | 4428 | 2858 | 5692 | 5292 | 4 | 2927 | 4622 | 4907 | 4716 |
| 2 | 4442 | 4428 | 5324 | 7 | 5393 | 3323 | 5036 | 7 | 4792 | 4640 |
| 3 | 4442 | 4414 | 5724 | 7 | 5425 | 4820 | 5159 | 0 | 4676 | 4532 |
| 4 | 4442 | 0 | 5580 | 2729 | 5310 | 5249 | 5000 | 3236 | 7 | 4453 |
| 5 | 4442 | 0 | 5623 | 5710 | 4 | 5080 | 4849 | 5044 | 4 | 4450 |
| 6 | 4442 | 2959 | 5648 | 5710 | 4 | 4612 | 3802 | 5198 | 3265 | 4460 |
| 7 | 4442 | 5224 | 5548 | 5663 | 3312 | 4385 | 4018 | 5058 | 5101 | 4460 |
| 8 | 4428 | 5710 | 7 | 5681 | 5137 | 4536 | 4288 | 4918 | 5198 | 7 |
| 9 | 4442 | 5512 | 7 | 5706 | 5152 | 4655 | 4568 | 3334 | 5072 | 0 |
| 10 | 4442 | 5580 | 2786 | 7 | 5022 | 4810 | 4784 | 3438 | 4889 | 3053 |
| 11 | 4428 | 5548 | 5638 | 7 | 5166 | 4907 | 4831 | 3762 | 3377 | 5130 |
| 12 | 4428 | 5263 | 5695 | 2686 | 5209 | 4950 | 4824 | 4180 | 3550 | 5184 |
| 13 | 4428 | 5008 | 5638 | 4871 | 5198 | 4 | 4792 | 4547 | 3838 | 5044 |
| 14 | 4428 | 7 | 5652 | 5159 | 5098 | 4 | 4752 | 4867 | 4201 | 4856 |
| 15 | 4428 | 4 | 5677 | 4975 | 4 | 0 | 4694 | 4946 | 4579 | 3791 |
| Average Outflow | 4436 | 3605 | 4493 | 3640 | 4048 | 3422 | 4554 | 3810 | 3830 | 3918 |
| Overall Average Outflow | 3974 | | | | | | | | | |

densities obtained using current FREFLO, modified FREFLO, and FRECON. The volumes are the instantaneous flow rates leaving the downstream boundary of the section and densities are the average section density at the end of the given simulation time.

The results in Tables 4 through 6 show that all three simulations indicate that traffic volume is at (or near) capacity on Sections 6 through 10, as expected. For sections upstream of Section 6, however, different patterns of output volume were

generated by the three programs. Note that the simulation results with current FREFLO shown here differ somewhat from the results presented by Babcock et al. (4) in their comparison of FRECON and FREFLO because some modifications (3) have been incorporated into FREFLO since that time.

With the current FREFLO, the volume allowed to enter a congested section decreases gradually to the capacity of the bottleneck and follows an oscillating pattern thereafter (Sections 4 and 5 in Table 4). That is, the output volume fluctuates

TABLE 8 SECTION DENSITY (vehicles/lane-mile)—CURRENT FREFLO

| Time (min.) | Section | | | | | | | | | |
|----------------|---------|------|------|-------|-------|-------|------|------|------|------|
| | 1 | 2 | 3 | 4 | 5 | 6 | 7 | 8 | 9 | 10 |
| 1 | 27.2 | 27.2 | 27.3 | 27.7 | 33.7 | 105.7 | 72.0 | 57.6 | 48.9 | 43.8 |
| 2 | 27.2 | 27.2 | 27.3 | 27.9 | 38.0 | 130.4 | 80.2 | 63.8 | 54.4 | 49.0 |
| 3 | 27.2 | 27.2 | 27.4 | 28.6 | 48.8 | 146.0 | 85.3 | 68.9 | 59.3 | 54.0 |
| 4 | 27.2 | 27.3 | 27.5 | 30.7 | 76.9 | 144.0 | 87.4 | 72.1 | 63.6 | 58.8 |
| 5 | 27.2 | 27.3 | 27.6 | 32.8 | 96.6 | 147.9 | 89.0 | 63.9 | 65.9 | 62.0 |
| 6 | 27.2 | 27.3 | 27.8 | 35.5 | 118.6 | 152.2 | 91.6 | 76.6 | 68.9 | 64.7 |
| 7 | 27.2 | 27.4 | 28.5 | 50.1 | 148.9 | 126.0 | 88.0 | 76.9 | 70.8 | 67.8 |
| 8 | 27.3 | 27.5 | 31.4 | 83.9 | 151.6 | 121.0 | 91.1 | 79.3 | 73.2 | 70.3 |
| 9 | 27.3 | 27.7 | 33.5 | 105.5 | 142.7 | 125.6 | 90.6 | 80.9 | 76.0 | 73.6 |
| 10 | 27.4 | 27.9 | 36.4 | 124.4 | 151.1 | 119.2 | 91.2 | 82.9 | 78.2 | 75.9 |

TABLE 9 SECTION DENSITY (vehicles/lane-mile)—MODIFIED FREFLO

| Time (min.) | Section | | | | | | | | | |
|----------------|---------|-------|-------|-------|-------|-------|------|------|------|------|
| | 1 | 2 | 3 | 4 | 5 | 6 | 7 | 8 | 9 | 10 |
| 1 | 27.2 | 27.2 | 27.3 | 27.7 | 34.8 | 115.0 | 74.4 | 58.7 | 49.4 | 43.9 |
| 2 | 27.2 | 27.3 | 27.5 | 29.0 | 82.7 | 103.6 | 79.7 | 63.5 | 54.5 | 49.2 |
| 3 | 27.2 | 27.3 | 27.7 | 32.6 | 78.8 | 117.5 | 78.3 | 65.6 | 58.5 | 53.5 |
| 4 | 27.2 | 27.3 | 29.6 | 70.3 | 87.3 | 99.7 | 74.9 | 68.7 | 61.4 | 57.0 |
| 5 | 27.3 | 27.6 | 30.7 | 120.4 | 115.9 | 128.2 | 82.5 | 69.1 | 62.7 | 59.5 |
| 6 | 27.3 | 27.7 | 31.5 | 109.6 | 146.3 | 87.4 | 85.3 | 71.1 | 64.2 | 61.0 |
| 7 | 29.5 | 36.9 | 74.4 | 79.8 | 91.2 | 119.1 | 80.8 | 68.9 | 63.5 | 61.5 |
| 8 | 32.8 | 59.3 | 88.7 | 81.8 | 87.9 | 109.2 | 80.2 | 79.3 | 64.6 | 61.8 |
| 9 | 33.1 | 117.2 | 106.0 | 71.9 | 85.7 | 104.1 | 80.5 | 71.0 | 65.5 | 63.3 |
| 10 | 44.4 | 81.0 | 153.9 | 115.4 | 63.9 | 107.8 | 79.6 | 71.2 | 67.5 | 64.5 |

around the capacity of the bottleneck. The oscillations in output volume within each time step are substantial.

The simulation results obtained from FRECON using a spatial step size of 0.01 mi indicate that the output volume from a section upstream of a congested section decreases gradually to the capacity of the bottleneck and remains at that level thereafter with virtually no oscillations (Sections 4 and 5 in Table 5). This implies a complete absence of turbulence at a bottleneck location.

With modified FREFLO, an interesting pattern is revealed as shown in Table 6. The instantaneous volumes entering the congested Sections 2 through 5 upstream of the bottleneck vary widely from zero to above capacity. These oscillations represent the realistic stop-and-go conditions in these sections.

Volumes leaving Section 5 during each 4-sec time slice over the 10-min period are given in Table 7. During the first 72 sec, there are no perturbations in flow because the congestion in Section 6 has not yet propagated upstream to Section 5. Subsequently, the outflow exhibits short-term oscillatory behavior. Observe that the volume leaving Section 5, as tabulated for each minute in Table 6, is actually the output volume during the 15th time slice in each minute, as given in Table 7. The 1-min averaged volumes and the overall 10-min averaged volume are

also given in Table 7. The 1-min averages oscillate around the bottleneck capacity, while the long-term, 10-min average of 3,974 vph approximates the bottleneck capacity of 4,000 vph. Thus, the modified FREFLO not only provides a realistic pattern of turbulent flow upstream of the bottleneck but is also able to maintain the desired level of throughput.

The section densities given in Tables 8 and 9 and Figure 5 show the spread of congestion upstream of Section 6 and the presence of an acceleration region downstream in all three simulations.

The simulated section densities under the two versions of FREFLO are similar and are typical for congested conditions (Tables 8 and 9). Although densities on the congested Section 6 for the current FREFLO (Table 8) are somewhat higher than the density normally observed on congested freeways (100–120 vehicles per lane-mile), they are not as high as those computed in the nonlinear test network (Table 1). Note, however, that the modified version (Table 9) propagates disturbances upstream more rapidly than the current version, for reasons given earlier.

The densities on congested sections under FRECON are in the range of 120 to 1,000 vehicles per lane-mile (3). Because

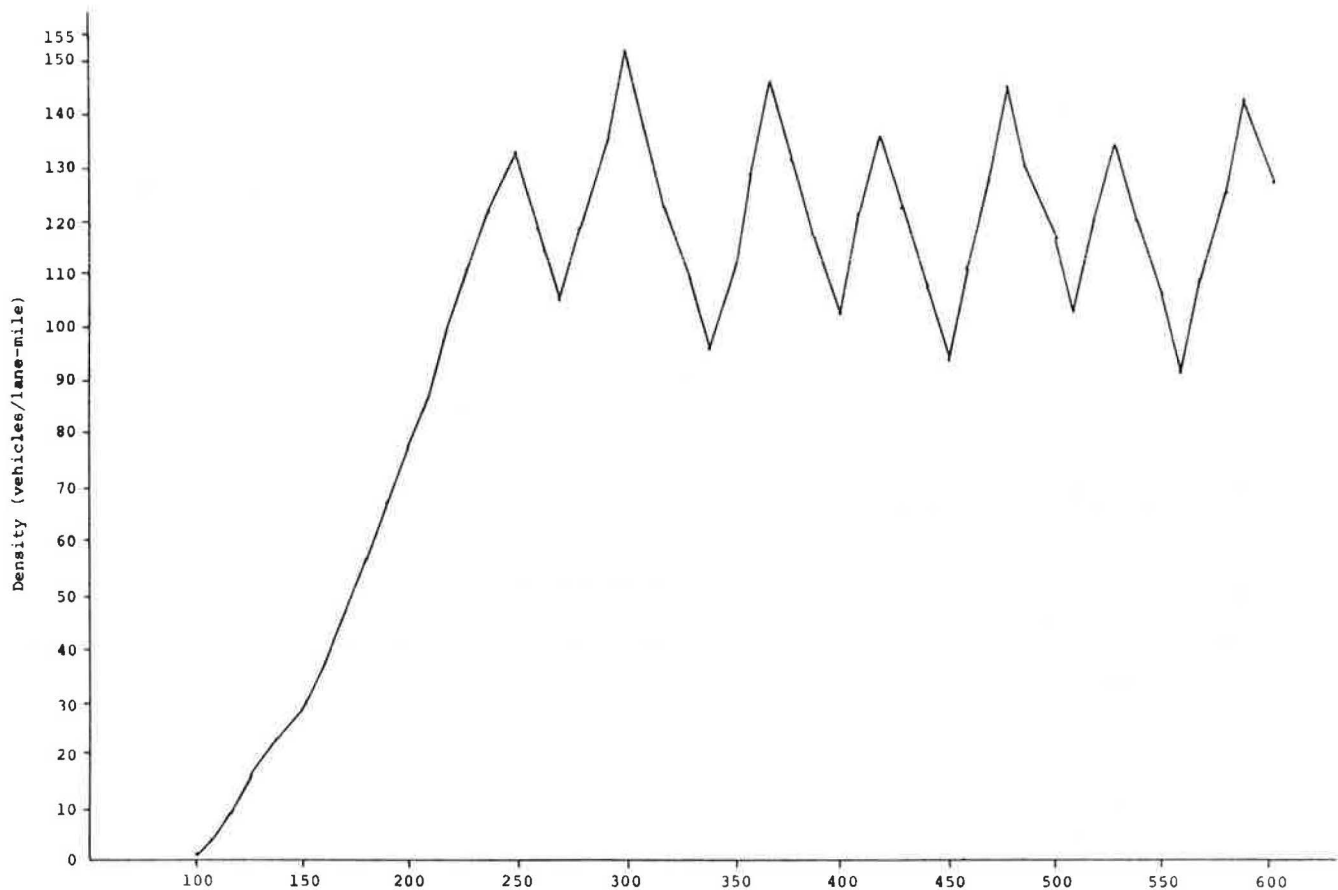


FIGURE 5 Density pattern on a congested section—modified FREFLO.

specific values of densities are not given, no evaluation of the densities produced by this model can be made.

The detailed history of density on a congested section under modified FREFLO is shown in Figure 5. This density gradually increases to the congested density level and oscillates thereafter, reflecting turbulent flow conditions. The amplitude and frequency of these oscillations vary depending on the section length, time slice duration, and outflow rate from feeder link and on whether this link is simulated before its feeder link(s).

CONCLUSIONS

Modifications were introduced to extend the ability of FREFLO to realistically simulate congested conditions for freeway sections of virtually any geometry. Tests of this modified FREFLO model reveal that it is able to:

- Produce values of densities that are much closer to those actually experienced on congested freeway sections,
- Propagate the effects of congestion to upstream sections in a timely manner,
- Produce a realistic stop-and-go pattern of flow entering congested sections, and
- Describe traffic within a diverging freeway section where one branch is congested and the other is not.

With modified FREFLO, the simulation results for the networks of the departments of transportation in Utah and Kansas, and some other test networks, have also been quite satisfactory. The results appear to be quantitatively, as well as qualitatively, accurate. The model is fully responsive to severe and to moderate incidents that block lanes for specified periods of time. The computational performance of FREFLO is not degraded and remains as user-friendly as it was previously.

These modifications have now been introduced as a permanent feature of FREFLO. FREFLO is available under a limited distribution from FHWA.

ACKNOWLEDGMENTS

This research was sponsored by FHWA. The authors wish to thank David Gibson of FHWA for his continued support of their efforts.

REFERENCES

1. H. J. Payne. FREFLO: A Macroscopic Simulation Model of Freeway Traffic. In *Transportation Research Record 722*, TRB, National Research Council, Washington, D.C., 1979, pp. 68-77.
2. H. J. Payne. *Calibration and Validation of FREFLO, Vol. I: User*

- Calibration Procedures and Supporting Data Analysis*. VERAC Report R-001-82. VERAC, Inc., San Diego, Calif.; FHWA, U.S. Department of Transportation, 1981.
3. P. S. Babcock, D. M. Auslander, M. Tomizuka, and A. D. May. Role of Adaptive Discretization in a Freeway Simulation Model. In *Transportation Research Record 971*, TRB, National Research Council, Washington, D.C., 1984, pp. 80-92.
 4. E. Lieberman. Integrated Traffic Simulation Model, Phase I, Vol. 1: Executive Summary. Report FHWA/RD-80/086. FHWA, U.S. Department of Transportation, Dec. 1979.
 5. H. J. Payne. Models of Freeway Traffic and Control. In *Simulation Council Proceedings, Mathematics of Public Systems*, Vol. 1, 1971, pp. 51-61.
 6. E. Lieberman, S. Nguyen, W. McShane, and C. Berger. *Analytical Developments for TRAFLO*. Report FHWA-RD-80-115. FHWA, U.S. Department of Transportation, 1982.
 7. A. K. Rathi. *FREFLO Enhancement*. KLD Associates, Inc., Huntington Station, N.Y., Nov. 1985.

Publication of this paper sponsored by Committee on Traffic Flow Theory and Characteristics.

Some Measurements of Robertson's Platoon Dispersion Factor

KAY W. AXHAUSEN AND HANS-GEORG KÖRLING

At the core of TRANSYT, the platoon dispersion model of Robertson is probably the most widely used traffic model in the world. In spite of its wide use, only a relatively small number of studies have tried to calibrate the model for a range of traffic conditions. The default values of the TRANSYT handbooks provide the only information on the value of the dispersion factor available to most users. In the first section of the paper, the sensitivity of the TRANSYT results to the dispersion value is shown. Next, available information on the model is summarized and the results are classified. In the last section of the paper, the results of measurements taken in Karlsruhe and in Pforzheim, West Germany, are reported. The experimental design of the sites was selected to determine the influence of the gradient and the number of lanes on the platoon dispersion.

Robertson's platoon dispersion model (1) forms the core of the widely used TRANSYT program in all its different versions (2, 3). Since the initial calibration of the model (1) there has been no major effort to calibrate it for a wide range of traffic situations. The studies undertaken to date to calibrate the model will be reported in the third section. In general, the low level of interest was based on the belief that the result of the optimization is only marginally affected by errors in the traffic model. The following section will present some evidence that this belief may be unwarranted in specific situations and could lead to grave errors. The aim of the small series of measurements reported in the last section is to gain a better basis for deter-

mination of value of the calibration factor for TRANSYT applications.

The model will be used with the following notation:

$$q'(i+t) = F * q(i) + (1-F) * q'(i+t-1)$$

with

$$t = \beta * T \quad F = \frac{1}{(1 + \alpha t)}$$

where

- T = average travel time between the observation points,
- t = average arrival time of the first vehicle of the platoon in intervals of n seconds,
- F = smoothing factor,
- α, β = calibration constants, and
- α_g = α calibrated with β fixed at 0.8.

SOME EVIDENCE OF THE EFFECTS OF VARIATIONS IN α_g

A real network of 11 nodes was used to study the effect of the variation of the dispersion factor. The network and the calibrated traffic data were available for the evening peak conditions. The calibration was part of a larger study involving TRANSYT as a tool to develop new signal plans for the city of